MOLECULAR AND CELLULAR BIOLOGY, June 2003, p. 3929–3935 Vol. 23, No. 11
0270-7306/03/$08.00+0 DOI: 10.1128/MCB.23.11.3929–3935.2003

The Histidine Triad Protein Hint Is Not Required for Murine Development or Cdk7 Function

Nina Korsisaari,[1] Derrick J. Rossi,[1] Keijo Luukko,[2] Kay Huebner,[3] Mark Henkemeyer,[4] and Tomi P. Mäkelä[1]*

Haartman Institute and Helsinki University Central Hospital, Biomedicum Helsinki, 00014 University of Helsinki, Finland[1]; Department of Anatomy and Cell Biology, University of Bergen, N-5009 Bergen, Norway[2]; Department of Microbiology and Immunology, Kimmel Cancer Center, Jefferson Medical College, Philadelphia, Pennsylvania 19107[3]; and Center for Developmental Biology, University of Texas Southwestern Medical Center, Dallas, Texas 75235-9133[4]

Received 11 October 2002/Returned for modification 2 December 2002/Accepted 4 March 2003

The histidine triad (HIT) protein Hint has been found to associate with mammalian Cdk7, as well as to interact both physically and genetically with the budding yeast Cdk7 homologue Kin28. To study the function of Hint and to explore its possible role in modulating Cdk7 activity in vivo, we have characterized the expression pattern of murine *Hint* and generated Hint-deficient (*Hint*$^{-/-}$) mice. *Hint* was widely expressed during mouse development, with pronounced expression in several neuronal ganglia, epithelia, hearts, and testes from embryonic day 15 onward. Despite this widespread expression, disruption of Hint did not impair murine development. Moreover, Hint-deficient mice had a normal life span and were apparently healthy. Histological examination of tissues with high *Hint* expression in wild-type animals did not show signs of abnormal pathology in *Hint*$^{-/-}$ mice. Functional redundancy within the HIT family was addressed by crossing *Hint*$^{-/-}$ mice with mice lacking the related HIT protein, Fhit, and by assaying the expression levels of the HIT protein gene family members *Hint2* and *Hint3* in *Hint*$^{+/+}$ and *Hint*$^{-/-}$ tissues. Finally, Cdk7 kinase activity and cell cycle kinetics were found to be comparable in wild-type and *Hint*$^{-/-}$ mouse embryonic fibroblasts, suggesting that Hint may not be a key regulator of Cdk7 activity.

The 14-kDa Hint protein was originally identified through biochemical purification and sequencing from bovine brain lysates (26). Hint belongs to a superfamily of histidine triad (HIT) hydrolases, which consists of small homodimerizing proteins characterized by conserved histidine residues (His-X-His-X-His-X-X, where X is a hydrophobic residue) near their carboxy-terminal ends (reviewed in reference 3). The Hint branch is the most widely conserved of the HIT superfamily, and Hint homologues are present in a wide variety of organisms in the metazoan, plant, fungus, and bacterial kingdoms. Fhit (for "fragile histidine triad") (24) represents a second branch of the HIT superfamily. Fhit has orthologues in many eukaryotes, including the budding yeast orthologue Hnt2 (Aph1) (4, 5). Recently, a protein named aprataxin (6, 21) was identified as a novel member of the first branch of the HIT protein superfamily. In contrast to Hint and Fhit, aprataxin contains a PANT (21) and a Zn finger domain in addition to the HIT domain.

Both FHIT and aprataxin have been implicated in disease. FHIT has been reported to function as a tumor suppressor in humans (reviewed in reference 11) and in mice, where *Fhit* deficiency was shown to increase sensitivity to tumor development (9, 32). Aprataxin was identified through mapping of the gene responsible for ataxia-ocular apraxia in humans (6, 21). To date, Hint has not been associated with human disease.

* Corresponding author. Mailing address: Haartman Institute and Helsinki University Central Hospital, Biomedicum Helsinki, P.O. Box 63, Haartmaninkatu 8, 00014 University of Helsinki, Finland. Phone: 358-9-19125555. Fax: 358-9-19125554. E-mail: tomi.makela@helsinki.fi.

HIT hydrolases hydrolyze unusual adenosine nucleotides. This activity is well characterized for Fhit and its budding yeast orthologue Hnt2, which are both diadenosine triphosphate (Ap3A) asymmetric hydrolases in vitro (1, 4, 17) and in vivo (5, 22, 28). The biological significance of the hydrolase activity of Fhit/Hnt2 remains to be characterized, as *hnt2* null yeast has no detectable phenotype (besides the accumulation of the Ap3A substrate) and Fhit hydrolase activity surprisingly does not correlate with its tumor suppressor function (29, 30). Hint also possesses in vitro affinity (10) and hydrolase activity towards small nucleotide compounds (17). The highest hydrolase activity has been measured for adenosine-5′-monophosphoramidate (APA/AMPNH$_2$) (2), which has been detected in vivo in unicellular green microalgae (8). Based on these biochemical experiments it has been speculated that Hint substrates would be of the form AMP-X, where X represents an unknown entity, and might even represent a protein moiety (3).

Hint was found to interact with the Cdk7 kinase in a two-hybrid screen (14). Moreover, a genetic interaction between the Hint budding yeast orthologue, Hnt1, and the Cdk7 orthologue, Kin28, was identified, suggesting a physiological relevance to the Cdk7-Hint association (2, 14). Cdk7 is the catalytic subunit of the trimeric Cdk7-cyclin H-MAT1 complex, which phosphorylates and activates cyclin-dependent kinases as a Cdk-activating kinase (reviewed in reference 12). Cdk7, cyclin H, and MAT1 also comprise the kinase subunit of the general transcription factor IIH, which is involved in regulation of transcription (reviewed in references 7 and 23).

Despite wide sequence conservation across kingdoms, the biological functions of Hint are largely unknown. In order to

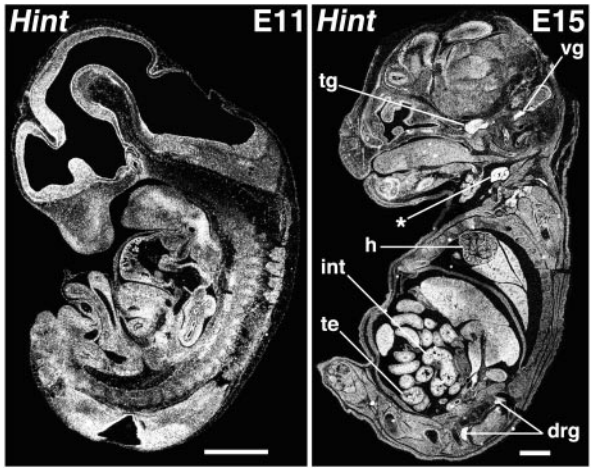

FIG. 1. Expression of *Hint* in E11 and E15 embryos. The localization of *Hint* mRNA was examined by in situ hybridization. Dark-field illuminations of sagittal sections are shown. Abbreviations: drg, dorsal root ganglia; h, heart; int, intestine; te, testis; tg, trigeminal ganglia; vg, vestibulo-cochlear ganglia. Asterisk, nonspecific staining of *Hint* probe in thymus. Bars, 1 mm.

study the function of Hint in a mammalian context, we characterized the expression pattern of *Hint*. We also generated *Hint*-deficient mice by targeted mutagenesis and analyzed the phenotype of these mice, in addition to studying the consequences of Hint loss for Cdk7 kinase activity.

MATERIALS AND METHODS

This investigation was approved by the Animal Welfare Committees of the Haartman Institute, University of Helsinki, and State Provincial Office of Southern Finland.

In situ hybridization. Mouse *Hint* (IMAGE 426110) and *Cdk7* (IMAGE 479857) open reading frames were used for in vitro transcription of ^{35}S-UTP-labeled antisense and sense probes. In situ hybridizations were performed as described in reference 31, with modifications (18).

Generation of Hint *flox* mice and PCR genotyping. A 129-SV mouse genomic library (Stratagene) was screened with a ^{32}P-labeled probe from a human *HINT* cDNA (GenBank accession no. U27143) corresponding to the open reading frame. Five overlapping clones were subjected to restriction mapping and sequencing, leading to the identification of two exons corresponding to nucleotides 163 to 267 and 268 to 575 of the murine *Hint* cDNA (GenBank accession no. AK002965) with large introns on both sides. A targeting vector was constructed by inserting 1.6-kb *Hin*dIII and 1.3-kb *Sma*I-*Hin*dIII genomic fragments flanking the targeted exons and a 1.5-kb *Hin*dIII-*Sma*I fragment containing the exons into the *loxP* conditional vector pDELBOY-3X (27). Homologous recombination was screened for by Southern blotting, and correctly targeted embryonic stem (ES) cell clones were injected into blastocysts from C57BL6 mice and subsequently implanted into pseudopregnant females. Several chimeric male offspring were found to transmit the targeted allele in the germ line. PCR genotyping of *Hint* alleles was achieved with the following primers: H7, 5′-GCA GGG AGC ACG CGG GAA GAG TCT GC; H10, 5′-CTG AAT ACA CAA GAA TGG GAA GAC C; and N4, 5′-GTC AGT TTC ATA GCC TGA AGA ACG. H7 and H10 amplify 240- and 330-bp fragments corresponding to the wild-type and *flox* alleles, respectively, while N4 and H10 amplify a 310-bp fragment corresponding to the null allele. PCR genotyping of the *Fhit* mice was achieved with the following primers: FHIT for, 5′-CTT GAA TCT AGG CTG CAT TCT AGC GAG; FHIT rev, 5′-GAT TCC TTG CTT ACC TTT TGG GGA TGG; and FHIT neo, 5′-TGG GCT CTA TGG CTT CTG AGG C. FHIT for and FHIT rev amplify a 450-bp fragment corresponding to the wild-type allele, while FHIT rev and FHIT neo amplify a 280-bp fragment corresponding to the null allele. PCRs were performed in a thermocycler by heating the reaction mixture at 95°C for 5 min followed by 35 cycles of 95°C for 50 s, 58°C for 50 s, and 72°C for 50 s.

Histology. For histological hematoxylin or hematoxylin-eosin staining, tissues were fixed overnight in 4% paraformaldehyde, dehydrated, and embedded in paraffin. Sections (7 μm) were deparaffinized, rehydrated, and histologically stained according to standard protocols.

Primary MEF culturing and analysis of cell cycle kinetics. Mouse embryonic fibroblasts (MEFs) were prepared from embryos at day 14 of embryogenesis (E14) according to standard protocols, and genotypes were determined by PCR. For serum starvation experiments, cultures of primary *Hint*$^{+/+}$ and *Hint*$^{-/-}$ MEFs were seeded onto duplicate 24-well plates at a density of 5×10^4 cells/well in Dulbecco's modified Eagle medium supplemented with 15% fetal bovine serum followed by induction of G_0 by withdrawal of serum for >48 h. Stimulation to reenter the cell cycle was performed by addition of 15% serum for 2, 8, 14, 16, 20, or 24 h. [*methyl*-^{3}H]thymidine (ICN) was introduced for the final 2 h of the culture at 2 μCi/ml of medium. After the [^{3}H]thymidine pulse, cells were washed twice with ice-cold phosphate-buffered saline and once with ice-cold 5% trichloroacetic acid and then fixed with a 30-min incubation in 5% trichloroacetic acid. After four washes with H_2O, cells were lysed in 0.5 M NaOH and analyzed by scintillation counting.

Western blotting analysis, immunoprecipitation, and kinase activity assay. Cultures of primary *Hint*$^{+/+}$ and *Hint*$^{-/-}$ MEFs were lysed in ELB buffer (150 mM NaCl, 50 mM HEPES [pH 7.4], 5 mM EDTA, 0.1% CA-630) with 10 mM β-glycerophosphate, 1 μg of leupeptin per ml, 12.5 μg of aprotinin per ml, 0.5 mM phenylmethylsulfonyl fluoride, and 1 mM dithiothreitol added, or similarly in ELB buffer with 300 mM KCl (omitting NaCl). For Western blotting analysis with RNA polymerase II (Pol II) antibodies H5 and H14, cells were lysed in boiling Laemmli sample buffer followed by a brief sonication. Immunoprecipitation was performed with a rabbit polyclonal anti-Cdk7 antibody (19) or anti-Cdk2 antibody from ELB lysates, and in vitro kinase activity towards a glutathione *S*-transferase C-terminal domain (GST-CTD), GST-Cdk2, or histone H1 substrate was measured. Immunoprecipitation and total lysate samples were run

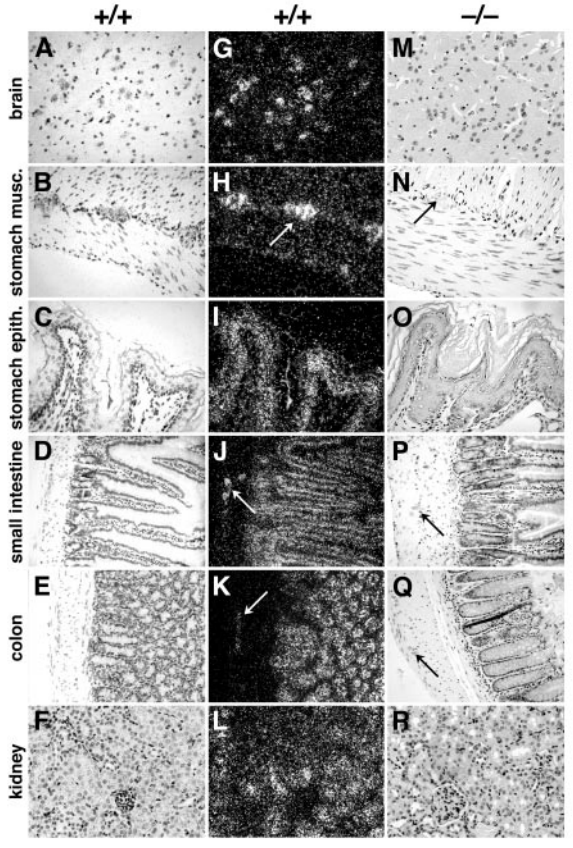

FIG. 2. *Hint*$^{-/-}$ animals do not display pathological changes in tissues that normally express *Hint* abundantly. Hematoxylin-stained sections of adult wild-type (+/+) tissues (A to F) with corresponding dark-field illuminations of in situ hybridization analysis (G to L) and comparable hematoxylin-stained tissues from Hint$^{-/-}$ animals (M to R) are shown. Arrows point to sympathetic nerves.

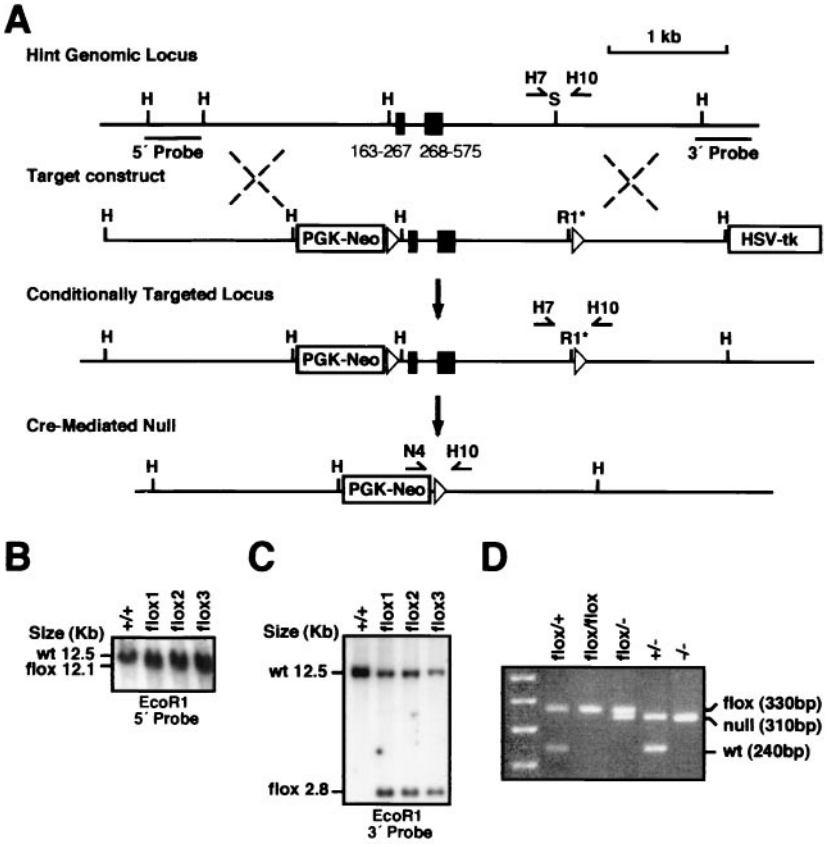

FIG. 3. Disruption of the murine *Hint* locus by targeted mutagenesis. (A) Partial genomic structure of the murine *Hint* gene showing exons 2 (nucleotides 163 to 267 of cDNA) and 3 (nucleotides 268 to 575) and a targeting vector used to generate the conditional targeted allele $Hint^{flox}$. The asterisk indicates that the *Eco*RI (R1) site has been introduced. Abbreviations: H, *Hin*dIII; S, *Sma*I. The PGK-Neo and HSV-tk cassettes are not drawn to scale. (B and C) Southern blotting analysis of the targeted ES cell lines. *Eco*RI-digested genomic DNA from wild-type and targeted ES cell lines flox1, flox2, and flox3 yielded the targeted 12.1-kb fragment and the 12.5-kb wild-type fragment with the 5′ probe (B) and the predicted 2.8-kb fragment in addition to the 12.5-kb wild-type fragment with the 3′ probe (C). (D) PCR genotyping of offspring bearing various genotypes that resulted from crossing $Hint^{flox/-}$ males to $Hint^{flox/-}$ or $Hint^{+/-}$ females. A 240-bp wild-type fragment, a 330-bp conditional (*flox*) fragment, and a 310-bp null allele fragment were amplified with the H7-H10 and N4-H10 primer pairs shown in panel A.

on sodium dodecyl sulfate-polyacrylamide gels with 7, 12, or 15% acrylamide. Primary antibodies were rabbit polyclonal antibodies against Hint (hPKCI, 1:1,000; a kind gift from Bernard Weinstein) (13), cyclin H (1:1,000, FL323; Santa Cruz), Mat1 (FL309, 1:1,000; Santa Cruz), and Cdk2 (sc-169, 1:1,000; Santa Cruz) and mouse monoclonal antibodies against Cdk7 (sc-7344, 1:500; Santa Cruz), actin (AC-40, 1:1,000; Sigma), and RNA Pol II epitopes H5, H14, and 8WG16 (all 1:500; Research Diagnostics). Secondary antibodies were horseradish peroxidase-conjugated anti-rabbit and anti-mouse immunoglobulin G (both 1:5,000; Chemicon) and anti-mouse immunoglobulin M (1:1,000; Zymed) antibodies.

Generation of *S. cerevisiae HNT1-HNT2* double disruptant. Generation and analysis of the *HNT1* disruptant strain have been described elsewhere (14). The *hnt2* (*aph1*) disruptant strain was a kind gift from Pierre Plateau (5). Mating, sporulation, and random spore analysis were performed according to standard procedures to produce a *hnt1*::*HIS3*; *hnt2*::*TRP1* double-mutant haploid strain, identified by auxotrophy analysis and PCR genotyping.

Generation and analysis of $Hint^{-/-}$; $Fhit^{-/-}$ mice. Fhit-deficient mice have been described (9). Cohorts of $Hint^{+/-}$; $Fhit^{-/-}$ and $Hint^{-/-}$; $Fhit^{-/-}$ littermates were generated and maintained on a mixed genetic background and aged. Careful necropsy and histological analysis of the stomach, small intestine, colon, ovary or testis, liver, kidney, spleen, pancreas, brain, and blood was performed at 18 months of age. The skin was palpated for detection of sebaceous tumors.

RNA extraction and real-time PCR. Total RNA was extracted from snap-frozen, pulverized tissues (liver, kidney, spleen, lung, and brain) of $Hint^{+/+}$ and $Hint^{-/-}$ animals with a Qiagen RNeasy kit. Total RNA (0.6 to 3.0 μg) was used to generate cDNA with a reverse transcriptase cDNA synthesis kit (Invitrogen, Carlsbad, Calif.). Real-time PCR was performed with PCR reagents and a GeneAmp 5700 light-cycler detection system (Applied Biosystems, Foster City, Calif.). PCR was achieved with the following primers: *Hint* for1, 5′-CGG GAA GGA CAG TGA GCG; *Hint* rev1, 5′-ATC CCC AAC CTG CTT TAA CC; *Hint2* for3, 5′-AGG TCC GAG GAA ACG CAG; *Hint2* rev1, 5′-TGG CAG GTT TAG CCA GGT GG; *Hint3* for1, 5′-ATG GCT GAG AAG CAA GCG; *Hint3* rev1, 5′-AAC TTG TCC ATG GTT CAC; gapdh for1, 5′-TGT TCC TAC CCC CAA TGT GT, gapdh rev1, 5′-TGT GAG GGA GAT GCT CAG TG.

RESULTS AND DISCUSSION

Hint mRNA expression during mouse development and in adult mice. To characterize the spatial and temporal expression of murine *Hint*, we performed in situ hybridization analysis of embryonic and adult tissues. Developmental expression was analyzed systematically between E7 and E17.5. During the early gestational and midgestational embryonic stages (E7 to E13), a strong *Hint* signal was ubiquitous and largely correlated with cell density (Fig. 1). Gradually this pattern changed so that while a low level of *Hint* expression was maintained throughout the embryo, strong expression was detected in the peripheral sensory trigeminal, vestibulo-cochlear, and dorsal root ganglia (Fig. 1), suggesting expression in neuronal cells.

TABLE 1. Hyperplastic polyposis in *Hint*; *Fhit* animals[a]

Genotype	Age (mo)	Polyp size (mm)	No. of polyp-bearing mice/total
$Hint^{+/-}$; $Fhit^{-/-}$	17.9 ± 1.8	4.7 ± 1.1	9/12
$Hint^{-/-}$; $Fhit^{-/-}$	17.9 ± 1.9	4.8 ± 1.4	9/11

[a] Data are means ± standard deviations.

Prominent expression was also noted in the heart, the mucosal epithelium of the intestine, and the germ cells of the developing testis (Fig. 1) and to a lesser extent in the liver. In contrast, the expression of *Cdk7* was ubiquitous and evenly distributed at all developmental stages analyzed (unpublished data).

Hint expression was subsequently analyzed in adult tissues. As in the developing embryo, a low level of *Hint* mRNA was detected in all analyzed tissues while stronger expression of *Hint* was restricted to certain tissues. A coronal section of the brain at the rostral level revealed a high level of *Hint* mRNA in the pyramid cells within the caudate-putamen (Fig. 2G). Likewise, strong *Hint* expression was noted in the neurons of the myoenteric plexuses along the gastrointestinal tract (Fig. 2H, J, and K). In addition to these neural cell types, high *Hint* expression was also noted in the differentiated keratinized cells of the stratified epithelium of the stomach (Fig. 2I) as well as in the epithelial cells of the small intestine and the colon (Fig. 2J and K). *Hint* expression was also prominent in the proximal tubules of the kidney, whereas the expression of *Hint* was weaker in the glomeruli and in the distal tubules (Fig. 2L). These data are in line with previous reports on the expression levels of Hint protein in the brain, stomach, and kidney (13, 20). Hint expression in the adult testis continued to be most prominent in the germ cells, where the highest expression was found in the pachytene spermatocytes (unpublished data). Abundant ovarian expression was located in the maturing follicles and the egg cytosol (unpublished data).

The high expression of *Hint* in several neuronal and epithelial cell types suggested that Hint might be required for the development or the specific functions of these cell types.

Conditional disruption of murine Hint by targeted mutagenesis. In an attempt to characterize the physiological functions of the mammalian Hint, we generated a targeted disruption of *Hint* in mice. The strategy depicted in Fig. 3A involved flanking exons 2 and 3 of the murine *Hint* gene (http://www.ncbi.nlm.nih.gov/LocusLink/LocRpt.cgi?l=15254) with *loxP* sites to generate a conditional (*flox*) allele which upon Cre recombinase-mediated excision would yield a deletion of the

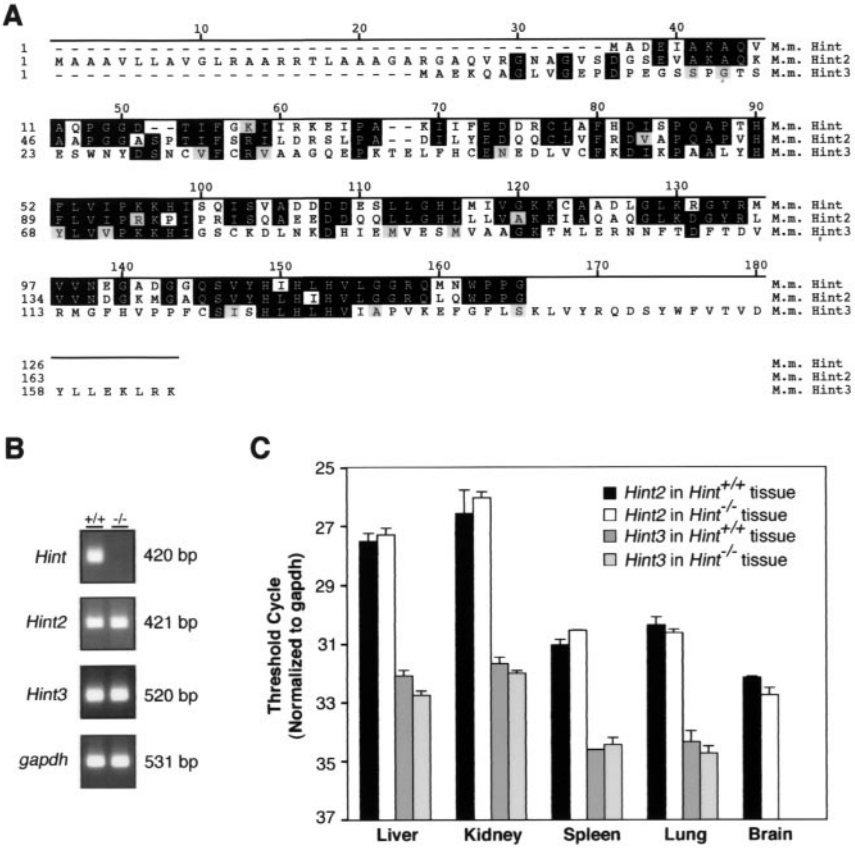

FIG. 4. HIT family sequence alignment and mRNA expression analysis. (A) Alignment of amino acid sequences of murine (M.m.) Hint, Hint2, and Hint3. Identity to the consensus sequence is marked with black boxes, and similarity is shown with gray boxes. (B) Specificity of real-time PCR strategy showing products of *Hint*, *Hint2*, *Hint3*, and *gapdh* amplified from cDNAs generated from total RNA extracted from $Hint^{+/+}$ and $Hint^{-/-}$ animals. (C) Real-time mRNA expression analysis of *Hint2* and *Hint3* showing the threshold cycle (linear phase of amplification, normalized to *gapdh* expression) in liver, kidney, spleen, lung, and brain from $Hint^{+/+}$ and $Hint^{-/-}$ animals. Note that *Hint3* expression was not detectable in the brain samples from $Hint^{+/+}$ or $Hint^{-/-}$ animals.

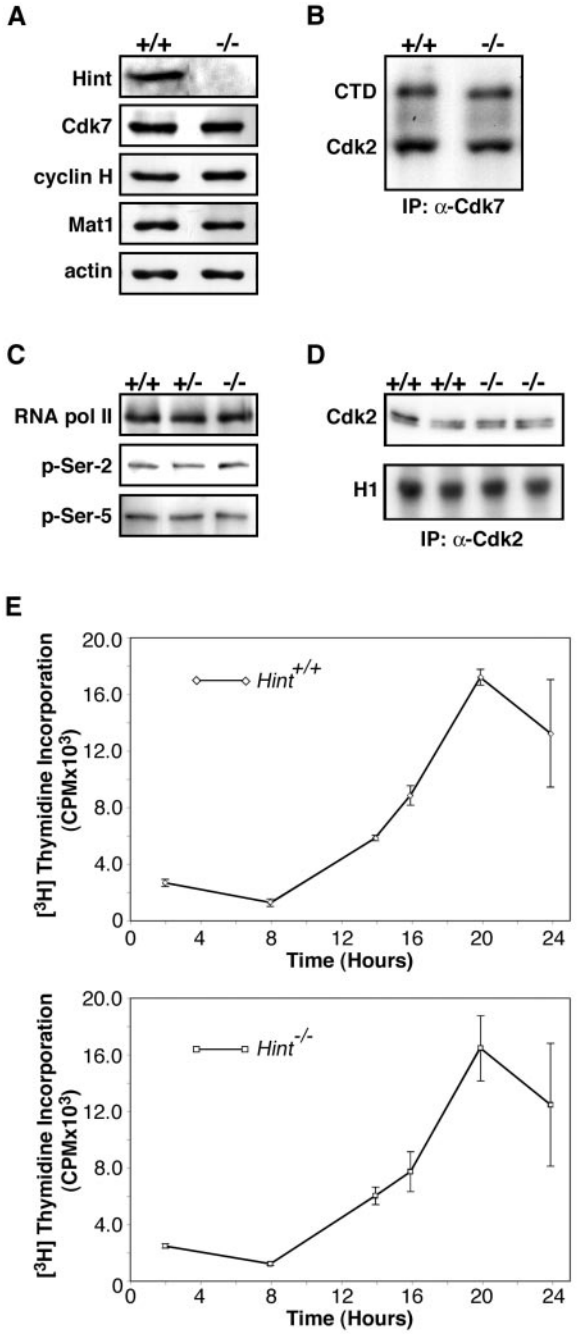

FIG. 5. Characterization of Cdk7 function in $Hint^{-/-}$ MEFs. (A) Western blotting analysis of endogenous Hint, Cdk7, cyclin H, Mat1, and actin from protein lysates from wild-type and *Hint* null MEFs. (B) In vitro Cdk7 kinase activity from *Hint* wild-type and *Hint* null MEFs assayed by using GST-CTD and GST-Cdk2 as substrates following anti-Cdk7 immunoprecipitation (IP). (C) Western blotting analysis from protein lysates of wild-type, *Hint* heterozygous, and *Hint* null MEFs with RNA Pol II large-subunit antibody 8WG16 recognizing nonphosphorylated Ser-2 (RNA Pol II), antibody H5, recognizing Pol II phosphorylated on serine 2 (p-Ser-2) of the CTD repeat, and antibody H14, recognizing Pol II phosphorylated on serine 5 (p-Ser-5) of the CTD repeat. (D) Western blot analysis of protein lysates from two independent cultures of wild-type and Hint null MEFs with a Cdk2 antibody recognizing total Cdk2 levels. In vitro Cdk2 kinase activity from unsynchronized *Hint* wild-type and *Hint* null MEFs was assayed by using histone H1 (H1) as a substrate following anti-Cdk2 immunoprecipitation. (E) [^{3}H]thymidine incorporation of wild-type and *Hint* null MEFs labeled at different times after release to G_1 by readdition of serum to starved cells. Standard deviations (error bars) originate from duplicates of three independent primary cultures for each genotype.

C-terminal 89 amino acids (aa) of the 125-aa Hint protein. The linearized targeting construct was electroporated into ES cells followed by positive (G418) and negative (ganciclovir) drug selection. Screening of 700 drug-resistant clones by Southern blotting analysis using external 5′ and 3′ probes indicated correct targeting in seven clones (Fig. 3B and C). ES cells from two of these clones were injected into blastocysts to generate mice bearing the conditionally targeted allele of *Hint* ($Hint^{flox}$).

Intercrossing $Hint^{flox/+}$ mice yielded F1 offspring bearing combinations of all the expected alleles (Fig. 3D). The $Hint^{flox/flox}$ mice were healthy and fertile, indicating that the conditional allele had no overt hypomorphic effects. To test the functionality of the *flox* allele in vivo, the $Hint^{flox/flox}$ conditional mice were crossed to a phosphoglycerate kinase 1 promoter-driven Cre deleter (PGK-Cre) mouse (a kind gift from Peter Lonai) (15), after which the recombined Hint null allele was observed in all offspring ($Hint^{+/-}$). Subsequent $Hint^{+/-}$ intercrosses produced $Hint^{-/-}$ offspring in Mendelian ratios (53 $Hint^{+/+}$, 127 $Hint^{+/-}$, and 55 $Hint^{-/-}$ offspring in a total of 235), indicating that *Hint* is not required for murine development despite the prominent expression of *Hint* during embryogenesis.

Lack of abnormalities in adult $Hint^{-/-}$ tissues. The results obtained from the expression study of embryonic and adult tissues, and the fact that *Hint* disruption was viable, prompted us to analyze the tissues exhibiting high *Hint* expression for pathological changes.

Histological analysis of the sympathetic nerves of the stomach, small intestine, and colon from the adult $Hint^{-/-}$ animals revealed no abnormalities (Fig. 2N, P, and Q). Moreover, the histology of the $Hint^{-/-}$ brain at the caudate-putamen was also normal (Fig. 2M). These histological observations were supported by the lack of symptoms indicative of autonomic nerve dysfunction.

Likewise, no abnormalities were noted in the several other tissues analyzed, including the epithelial cells of the gastrointestinal tract, the kidney, and the liver (Fig. 2O, P, Q, and R and unpublished data). Furthermore, fertility of $Hint^{-/-}$ males and females was comparable to that of wild-type animals, indicating no defects in reproductive functions or the production of the germ cells.

The normal development of the *Hint*-deficient mice and the lack of histological abnormalities in the tissues of the $Hint^{-/-}$ animals correlate with the natural life span observed for the $Hint^{-/-}$ animals, which frequently extended beyond 2 years. These data indicate that *Hint* is not an essential gene for long-term survival in the mouse. The lack of phenotypes in $Hint^{-/-}$ mice suggest that either the loss of Hint function is compensated for by another molecule(s) or the physiological functions of Hint are such that their malfunction does not manifest itself in nonchallenged animals in the laboratory environment.

Functional redundancy within the HIT family? The possibility of functional redundancy within the HIT family was first

investigated in the budding yeast *Saccharomyces cerevisiae*. It has been noted (2, 14) that yeast cells with deletions of the *Hint* orthologue *Hnt1* are viable. Disruption of the *Fhit* orthologue *Hnt2* in budding yeast also resulted in viable cells with no detected growth defects (5). To determine whether the lack of phenotype in these strains might be due to functional redundancy, we generated a double disruptant of the *S. cerevisiae Hint* and *Fhit* homologues. The *hnt1*Δ *hnt2*Δ strain was found to be viable with no apparent growth defects (unpublished data), suggesting that the lack of phenotype in both single disruptants was not due to functional redundancy between *Hnt1* and *Hnt2*.

To investigate the possibility of redundancy between *Hint* and *Fhit* in mice, we crossed the $Hint^{-/-}$ mice with *Fhit*-deficient mice (9). Analysis of the $Hint^{-/-}$; $Fhit^{-/-}$ double-mutant mice revealed that their development and longevity were comparable to those of wild-type animals. Cohorts of $Hint^{+/-}$; $Fhit^{-/-}$ and $Hint^{-/-}$; $Fhit^{-/-}$ littermates were then analyzed for phenotypes previously observed in *Fhit*-deficient mice (9, 32). As has been reported, we observed gastric hyperplastic polyp formation in our animals, although the polyp frequency, size, location, and histology did not differ between the two cohorts (Table 1 and unpublished data). A small number of extraintestinal tumors and neoplasias were also observed, including two lymphomas in the $Hint^{+/-}$; $Fhit^{-/-}$ cohort and one liver tumor in the $Hint^{-/-}$; $Fhit^{-/-}$ cohort. These results indicate that loss of Hint did not noticeably alter the tumor spectrum associated with Fhit loss. The differences in tumor frequency that were observed in our cohorts in comparison to those previously reported for the Fhit-deficient animals (32) may reflect differences in genetic background. In conclusion, these data do not support a functional redundancy between the murine Hint and Fhit.

Recently, two novel HIT family members, Hint2 and Hint3, that share sequence homology with Hint were identified (GenBank accession numbers AF356515 and AK002482, respectively). The murine *Hint2* encodes a 163-aa protein with 61.3% sequence identity to Hint, while *Hint3* encodes a 165-aa protein with 21.3% sequence identity to Hint (Fig. 4A). These data suggest that Hint2 (and to a lesser degree Hint3) may be more likely to compensate for the loss of Hint activity in $Hint^{-/-}$ mice than Fhit, which shares only 18.5% sequence identity to Hint (alignment starting at Hint aa 17).

Evidence suggesting that related proteins of a family might functionally compensate for the loss of another can be provided by noting differences in expression of remaining family members (16). To determine if the mRNA expression of either *Hint2* or *Hint3* was deregulated in response to Hint loss in $Hint^{-/-}$ tissues, we performed reverse transcription on RNAs isolated from tissues of $Hint^{+/+}$ and $Hint^{-/-}$ animals followed by real-time PCR (Fig. 4B and C). We found that while the expression of neither *Hint2* or *Hint3* was dramatically altered in the $Hint^{-/-}$ tissues compared to the $Hint^{+/+}$ tissues, minor tissue-specific differences in expression were noted (Fig. 4C). Of these, the most significant was a 1.4-fold increase in *Hint2* expression in the spleen of $Hint^{-/-}$ mice (corresponding to a linear phase of amplification [threshold cycle] of 31.04 [standard deviation, 0.19] in $Hint^{+/+}$ spleen compared to 30.55 [standard deviation, 0.02] in $Hint^{-/-}$ spleen). Taken together, these results indicate that if Hint2 or Hint3 compensates for the loss of Hint, this redundancy is not associated with a dramatic concomitant change in expression.

Lack of evidence for the regulation of Cdk7 functions by Hint. The generation of $Hint^{-/-}$ mice allowed us to explore whether the lack of Hint in mammalian cells had any impact on the functions ascribed to the Cdk7 kinase and its associated proteins. These involve both phosphorylation and activation of the major cell cycle cyclin-dependent kinases (reviewed in reference 12), as well as regulation of transcription as part of TFIIH through a variety of mechanisms, including phosphorylation of the heptapeptide Y-S-P-T-S-P-S repeat sequence of the CTD of the large subunit of Pol II (reviewed in reference 23).

It was previously shown that disruption of the Cdk7-associated molecule, Mat1, resulted in early embryonic lethality of Mat1-deficient mice (27). In contrast, the Hint-deficient mice showed no apparent embryonic or adult phenotype, suggesting that loss of Hint activity did not result in a dramatic alteration in Cdk7 function. To investigate this issue in more detail, primary MEFs were generated from control and $Hint^{-/-}$ embryos. Western blotting analysis of lysates prepared from wild-type ($Hint^{+/+}$) or $Hint^{-/-}$ MEFs demonstrated that the protein levels of Cdk7, cyclin H, and Mat1 were comparable in cells of both genotypes, while the Hint protein was absent from the $Hint^{-/-}$ MEFs, as expected (Fig. 5A). When the kinase activity of Cdk7 was analyzed following immunoprecipitation of the kinase complex from both wild-type and $Hint^{-/-}$ MEFs, no change was observed in the ability of Cdk7 to phosphorylate either a GST-CTD or a GST-Cdk2 substrate (Fig. 5B). We then assayed the in vivo phosphorylation status of Pol II using antibodies recognizing phosphospecific epitopes of the CTD (25). These results indicated that loss of Hint did not alter the in vivo phosphorylation of Pol II at either serine 2 or serine 5 of the CTD heptapeptide repeat (Fig. 5C). Moreover, we found that the total levels of Cdk2 were unaltered in the Hint-deficient cells and that the kinase activity of Cdk2 towards histone H1 was not altered in $Hint^{-/-}$ MEFs (Fig. 5D). To more directly assay Cdk2 activity and cell cycle kinetics, several independent cultures of primary $Hint^{+/+}$ and $Hint^{-/-}$ MEFs were serum starved to arrest the cells in G_0, followed by the return of serum. S-phase entry was then monitored by measuring the incorporation of [^{3}H]thymidine into the DNA of cells that reentered the cell cycle (Fig. 5E). This experiment revealed that $Hint^{+/+}$ and $Hint^{-/-}$ MEFs displayed comparable cell cycle kinetics, providing further evidence that loss of Hint does not compromise Cdk7 or Cdk2 activity.

ACKNOWLEDGMENTS

We thank Peter Lonai for the PGK-Cre mice, Pierre Plateau for the *HNT2 S. cerevisiae* disruptant strain, and Bernard Weinstein for Hint antibodies. Ari Ristimäki, Matti Haltia, and Kirsi Sainio are acknowledged for consultation. Birgitta Tjäder, Susanna Räsänen, and Sanna Kihlberg are acknowledged for excellent technical assistance.

N.K. and D.J.R contributed equally to this work.

This study was supported by grants from Biocentrum Helsinki, the Finnish Cancer Organization, the Sigrid Juselius Foundation, TEKES, and the Academy of Finland. N.K. was supported by the Helsinki Graduate School in Biotechnology and Molecular Biology, and D.J.R. was supported by the Helsinki Biomedical Graduate School.

REFERENCES

1. **Barnes, L. D., P. N. Garrison, Z. Siprashvili, A. Guranowski, A. K. Robinson, S. W. Ingram, C. M. Croce, M. Ohta, and F. Huebner.** 1996. Fhit, a

putative tumor suppressor in humans, is a dinucleoside 5′,5′′′-P-1,P-3-triphosphate hydrolase. Biochemistry **35:**11529–11535.
2. **Bieganowski, P., P. N. Garrison, S. C. Hodawadekar, G. Faye, L. D. Barnes, and C. Brenner.** 2002. Adenosine monophosphoramidase activity of Hint and Hnt1 supports function of Kin28, Ccl1, and Tfb3. J. Biol. Chem. **277:** 10852–10860.
3. **Brenner, C.** 2002. Hint, Fhit, and GalT: function, structure, evolution, and mechanism of three branches of the histidine triad superfamily of nucleotide hydrolases and transferases. Biochemistry **41:**9003–9014.
4. **Brevet, A., J. Chen, M. Fromant, S. Blanquet, and P. Plateau.** 1991. Isolation and characterization of a dinucleoside triphosphatase from *Saccharomyces cerevisiae*. J. Bacteriol. **173:**5275–5279.
5. **Chen, J., A. Brevet, S. Blanquet, and P. Plateau.** 1998. Control of 5′,5′-dinucleoside triphosphate catabolism by APH1, a *Saccharomyces cerevisiae* analog of human FHIT. J. Bacteriol. **180:**2345–2349.
6. **Date, H., O. Onodera, H. Tanaka, K. Iwabuchi, K. Uekawa, S. Igarashi, R. Koike, T. Hiroi, T. Yuasa, Y. Awaya, T. Sakai, T. Takahashi, H. Nagatomo, Y. Sekijima, I. Kawachi, Y. Takiyama, M. Nishizawa, N. Fukuhara, K. Saito, S. Sugano, and S. Tsuji.** 2001. Early-onset ataxia with ocular motor apraxia and hypoalbuminemia is caused by mutations in a new HIT superfamily gene. Nat. Genet. **29:**184–188.
7. **Egly, J. M.** 2001. The 14th Datta Lecture. TFIIH: from transcription to clinic. FEBS Lett. **498:**124–128.
8. **Fankhauser, H., G. A. Berkowitz, and J. A. Schiff.** 1981. A nucleotide with the properties of adenosine 5′ phosphoramidate from Chlorella cells. Biochem. Biophys. Res. Commun. **101:**524–532.
9. **Fong, L. Y., V. Fidanza, N. Zanesi, L. F. Lock, L. D. Siracusa, R. Mancini, Z. Siprashvili, M. Ottey, S. E. Martin, T. Druck, P. A. McCue, C. M. Croce, and K. Huebner.** 2000. Muir-Torre-like syndrome in Fhit-deficient mice. Proc. Natl. Acad. Sci. USA **97:**4742–4747.
10. **Gilmour, J., N. Liang, and J. M. Lowenstein.** 1997. Isolation, cloning and characterization of a low-molecular-mass purine nucleoside- and nucleotide-binding protein. Biochem. J. **326:**471–477.
11. **Huebner, K., and C. M. Croce.** 2001. FRA3B and other common fragile sites: the weakest links. Nat. Rev. Cancer **1:**214–221.
12. **Kaldis, P.** 1999. The cdk-activating kinase (CAK): from yeast to mammals. Cell. Mol. Life Sci. **55:**284–296.
13. **Klein, M. G., Y. Yao, E. D. Slosberg, C. D. Lima, Y. Doki, and I. B. Weinstein.** 1998. Characterization of PKCI and comparative studies with FHIT, related members of the HIT protein family. Exp. Cell Res. **244:**26–32.
14. **Korsisaari, N., and T. P. Mäkelä.** 2000. Interactions of Cdk7 and Kin28 with Hint/PKCI-1 and Hnt1 histidine triad proteins. J. Biol. Chem. **275:**34837–34840.
15. **Lallemand, Y., V. Luria, R. Haffner-Krausz, and P. Lonai.** 1998. Maternally expressed PGK-Cre transgene as a tool for early and uniform activation of the Cre site-specific recombinase. Transgenic Res. **7:**105–112.
16. **Lam, E. W., J. Glassford, L. Banerji, N. S. Thomas, P. Sicinski, and G. G. Klaus.** 2000. Cyclin D3 compensates for loss of cyclin D2 in mouse B-lymphocytes activated via the antigen receptor and CD40. J. Biol. Chem. **275:**3479–3484.
17. **Lima, C. D., M. G. Klein, and W. A. Hendrickson.** 1997. Structure-based analysis of catalysis and substrate definition in the HIT protein family. Science **278:**286–290.
18. **Luukko, K., M. Moshnyakov, K. Sainio, M. Saarma, H. Sariola, and I. Thesleff.** 1996. Expression of neurotrophin receptors during rat tooth development is developmentally regulated, independent of innervation, and suggests functions in the regulation of morphogenesis and innervation. Dev. Dyn. **206:**87–99.
19. **Mäkelä, T. P., J. D. Parvin, J. Kim, L. J. Huber, P. A. Sharp, and R. A. Weinberg.** 1995. A kinase-deficient transcription factor TFIIH is functional in basal and activated transcription. Proc. Natl. Acad. Sci. USA **92:**5174–5178.
20. **McDonald, J. R., U. Groschel-Stewart, and M. P. Walsh.** 1987. Properties and distribution of the protein inhibitor (Mr 17,000) of protein kinase C. Biochem. J. **242:**695–705.
21. **Moreira, M. C., C. Barbot, N. Tachi, N. Kozuka, E. Uchida, T. Gibson, P. Mendonca, M. Costa, J. Barros, T. Yanagisawa, M. Watanabe, Y. Ikeda, M. Aoki, T. Nagata, P. Coutinho, J. Sequeiros, and M. Koenig.** 2001. The gene mutated in ataxia-ocular apraxia 1 encodes the new HIT/Zn-finger protein aprataxin. Nat. Genet. **29:**189–193.
22. **Murphy, G. A., D. Halliday, and A. G. McLennan.** 2000. The Fhit tumor suppressor protein regulates the intracellular concentration of diadenosine triphosphate but not diadenosine tetraphosphate. Cancer Res. **60:**2342–2344.
23. **Oelgeschlager, T.** 2002. Regulation of RNA polymerase II activity by CTD phosphorylation and cell cycle control. J. Cell Physiol. **190:**160–169.
24. **Ohta, M., H. Inoue, M. G. Cotticelli, K. Kastury, R. Baffa, J. Palazzo, Z. Siprashvili, M. Mori, P. McCue, T. Druck, et al.** 1996. The FHIT gene, spanning the chromosome 3p14.2 fragile site and renal carcinoma-associated t(3;8) breakpoint, is abnormal in digestive tract cancers. Cell **84:**587–597.
25. **Patturajan, M., R. J. Schulte, B. M. Sefton, R. Berezney, M. Vincent, O. Bensaude, S. L. Warren, and J. L. Corden.** 1998. Growth-related changes in phosphorylation of yeast RNA polymerase II. J. Biol. Chem. **273:**4689–4694.
26. **Pearson, J. D., D. B. DeWald, W. R. Mathews, N. M. Mozier, H. A. Zurcher-Neely, R. L. Heinrikson, M. A. Morris, W. D. McCubbin, J. R. McDonald, E. D. Fraser, et al.** 1990. Amino acid sequence and characterization of a protein inhibitor of protein kinase C. J. Biol. Chem. **265:**4583–4591.
27. **Rossi, D. J., A. Londesborough, N. Korsisaari, A. Pihlak, E. Lehtonen, M. Henkemeyer, and T. P. Mäkelä.** 2001. Inability to enter S phase and defective RNA polymerase II CTD phosphorylation in mice lacking Mat1. EMBO J. **20:**2844–2856.
28. **Rubio-Texeira, M., J. M. Varnum, P. Bieganowski, and C. Brenner.** 2002. Control of dinucleoside polyphosphates by the FHIT-homologous HNT2 gene, adenine biosynthesis and heat shock in Saccharomyces cerevisiae. BMC Mol. Biol. **3:**7.
29. **Siprashvili, Z., G. Sozzi, L. D. Barnes, P. McCue, A. K. Robinson, V. Eryomin, L. Sard, E. Tagliabue, A. Greco, L. Fusetti, G. Schwartz, M. A. Pierotti, C. M. Croce, and K. Huebner.** 1997. Replacement of Fhit in cancer cells suppresses tumorigenicity. Proc. Natl. Acad. Sci. USA **94:**13771–13776.
30. **Werner, N. S., Z. Siprashvili, L. Y. Fong, G. Marquitan, J. K. Schroder, W. Bardenheuer, S. Seeber, K. Huebner, J. Schutte, and B. Opalka.** 2000. Differential susceptibility of renal carcinoma cell lines to tumor suppression by exogenous Fhit expression. Cancer Res. **60:**2780–2785.
31. **Wilkinson, D. G., and J. Green.** 1990. In situ hybridization and the three-dimensional reconstruction of serial sections, p. 155–171. *In* A. J. Copp and D. L. Cockroft (ed.), Postimplantation mammalian embryos: a practical approach. IRL Press, Oxford, England.
32. **Zanesi, N., V. Fidanza, L. Y. Fong, R. Mancini, T. Druck, M. Valtieri, T. Rudiger, P. A. McCue, C. M. Croce, and K. Huebner.** 2001. The tumor spectrum in FHIT-deficient mice. Proc. Natl. Acad. Sci. USA **98:**10250–10255.